Catalysis Letters 23 (1994) 369–376

Catalytic properties of various MgO catalysts for oxidative coupling of methane

Kaiji Zhen, Senzi Li, Yingli Bi, Xiangguang Yang

Department of Chemistry, Jilin University, Changchun 130023, PR China

and

Quan Wei

The Testing Center, Jilin University, Changchun 130023, PR China

Received 21 March 1993; accepted 7 August 1993

A series of MgO catalysts for the oxidative coupling of methane prepared by different methods have been investigated. Specific surface area, XRD and XPS measurement results reveal that at lower temperatures catalysts with larger specific surface area, larger lattice distortion, smaller crystal dimension, and higher amount of unsaturated coordinated surface oxygen give higher catalytic activity. However, if we compare the catalytic properties of the samples in terms of unit surface area, the dependence of catalytic properties of the samples will be different.

Keywords: Oxidative coupling of methane; magnesia; surface area

1. Introduction

In recent years considerable effort has been devoted to the oxidative coupling of methane due to the significance of theory and utilization. It is well known that Li-doped metal oxides possess higher selectivity and higher yield of C_2 hydrocarbons. However, it is difficult to solve the problem of deactivation for Li-containing oxide catalysts. As a result much attention has been paid to the alkaline earth and rare-earth oxides. MgO is considered as a better catalyst in our studies because of its relatively high activity and stability, especially at lower temperatures and higher GVHS. We examined various sorts of magnesia and found that their catalytic properties are quite different due to the difference of preparation methods. In this paper structural factors in the bulk of the catalysts have been investigated. Furthermore, their structural factors are correlated with their catalytic activity for the reaction.

2. Experimental

2.1. CATALYST PREPARATION

Sample A: Pure MgO produced by Merck.

Sample B: Prepared by decomposing $MgCO_3$ at 1173 K for 8 h.

Sample C: Prepared by decomposing $Mg(NO_3)_2 \cdot 6H_2O$ at 1173 K for 8 h.

Sample D: Obtained from magnesium ribbon. Magnesium strip was pretreated in dilute hydrochloric acid so as to get black oxide film on the surface prior to burning in pure O_2 and collecting the formed white powder.

Sample E: Prepared by $Mg(OH)_2$. 0.2 mol $Mg(NO_3) \cdot 6H_2O$ was dissolved in boiled deionized water nearly to saturation. Excessive ammonium hydroxide was added under intensive stirring at 343 K. The resulting slurry was washed and filtered several times followed by drying at 383 K for 8 h and calcining at 1173 K for 8 h.

Sample F: Prepared by $Mg_2(OH)_2CO_3$. 0.2 mol $Mg(NO_3) \cdot 6H_2O$ was dissolved in 100 ml water (solution A) and 0.4 mol ammonium hydrocarbonate in 500 ml water (solution B). Solution B was added to A under magnetic stirring. A white granular precipitate gradually formed. The obtained precipitate then was heated and stirred for 30 min, washed and filtered several times. Subsequently the catalyst was dried at 383 K for 8 h and calcined at 1173 K for 8 h.

2.2. CATALYST CHARACTERIZATION

(a) The catalytic reaction was carried out in a quartz fixed bed reactor (9 mm i.d.). The ratio of reactant gases is $CH_4 : O_2 : N_2 = 20 : 10 : 50$ ml/min. All the catalysts were pelletized and sieved to 20–60 mesh. 0.2 g catalyst was embedded for each run. In most cases the reaction temperature was set at 723–1073 K, the composition of the effluent gases was analyzed by means of a 2305 gas chromatograph manufactured in China by Beijing Analytical Instruments Factory, equipped with a flame ionization detector and a Porapak Q column.

(b) X-ray diffraction measurements were performed on a Shimadzu-3DX-X ray diffractometer with Cu K_α radiation and Ni filter. Lattice parameter and particle size of the samples were determined at a low scanning speed 1/4 °/min. Single crystal CaF_2 was used as standard reference and KCl was used as internal standard for lattice parameter measurements.

The following equations were employed:

lattice parameter :

$$a = \lambda(h^{*2} + k^{*2} + l^{*2})^{1/2}(2 \sin \theta)^{-1};$$

particle size :

$$D_{202} = k\lambda(\beta - \beta^0)^{-1}(\cos \theta)^{-1};$$

lattice distortion :

$$(\beta - \beta^0)^2 = (\cos^2 \theta) = (4/\pi^2)(\lambda/D)^2 + 32\langle\varepsilon^2\rangle\sin^2 2\theta,$$

where $\langle \varepsilon^2 \rangle$ represents the mean square lattice distortion of the crystal faced to the direction perpendicular to the $(h^* k^* l^*)$ plane.

(c) The specific surface area of the sample was determined by means of atmospheric and physical adsorption of air and calculated according to $S = \Delta P / m(A + BP)$, where P is the equilibrium pressure, m the amount of sample, ΔP the pressure difference under equilibrium of the sample before and after adsorption, and A and B are apparatus constants.

(d) Surface composition of samples was measured by using an Escalab MK II photoelectron spectrometer equipped with Mg K_α radiation source (12 kV, 20 mA). The residual pressure was 10^{-7} Pa during data collection. C_{1s} (284.6 eV) peak was used to calibrate the charge effect.

3. Results and discussion

Figs. 1, 2 and 3 show the CH_4 conversion, C_2 selectivity and C_2 yield of MgO catalysts at 773–1073 K respectively. From these figures it can be seen that there exists great disparity in catalytic properties for MgO catalysts prepared by different approaches, that only A and B are more selective for C_2 hydrocarbon formation at 823 K and that sample A gives the highest C_2 yield.

3.1. THE EFFECT OF SURFACE AREA ON THE CATALYTIC PROPERTIES

The dependence of CH_4 conversion and C_2 yield of the catalysts measured at 923 K on the surface area are shown in fig. 4. From fig. 4 one can see that CH_4 conversion and C_2 yield are in line with their specific surface areas, i.e., with an increase in surface area there is an increase in catalytic properties.

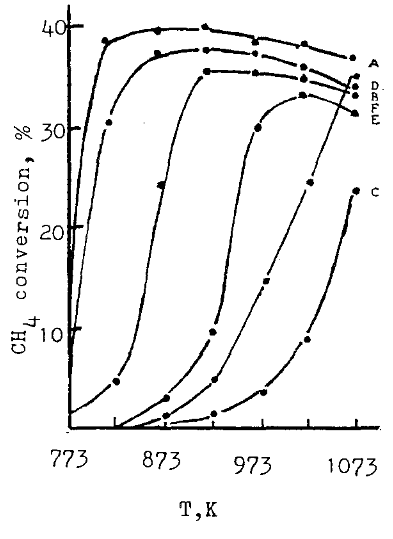

Fig. 1. Dependence of CH_4 conversion on reaction temperature.

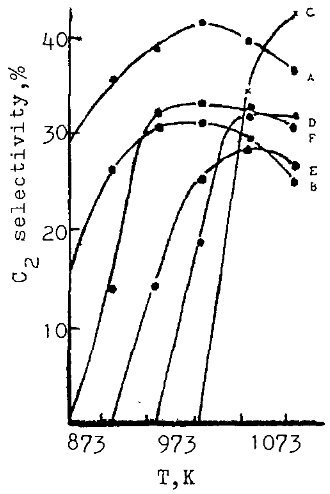

Fig. 2. Dependence of C_2 selectivity on reaction temperature.

In order to further understand the dependence of methane conversion and C_2 yield on surface area, we compared them in terms of the unit surface area of the samples by using the data given in fig. 4. One can find two points from fig. 5. (1) There exists an almost identical relation of change in methane conversion and C_2 yield per unit area with the specific surface area; (2) the catalysts with equal specific surface area exhibit almost equal methane conversion and C_2 yield for example, samples B and F (their specific surface areas are all about 25 m^2/g).

Comparing figs. 4 and 5 one can easily see that the dependences of total methane conversion and C_2 yield and the corresponding unit ones on specific surface area are quite different. Thus, it seems reasonable to consider the active surface of the samples.

Generally speaking, although preparation method and specific surface area

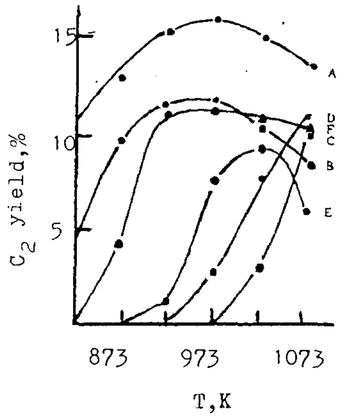

Fig. 3. Dependence of C_2 yield on reaction temperature.

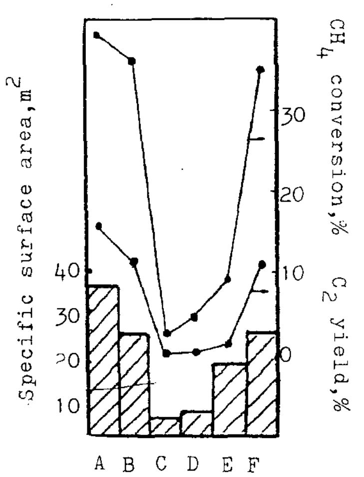

Fig. 4. Dependence of CH_4 conversion and C_2 yield on specific surface area.

influence the catalytic properties, the effect of the former, to some extent, is predominant. It is to say, if the specific area is almost equal, the catalytic properties are also the same in spite of the difference of preparation approaches.

As is well known, on the one hand, the larger the surface area, the more the active sites for methane coupling; on the other hand, over catalysts with larger surface area the collision probability of $CH_3\cdot$ radicals with the surface is increased, which results in the complete oxidation to CO_x. The same applies to the temperature dependence. Higher temperature will increase the rate of formation and desorption of $CH_3\cdot$ radicals, which is responsible for the formation of C_2 hydrocarbons. However, it may also fasten the rate of deep oxidation.

In case where the catalyst surface area is smaller and the reaction temperature

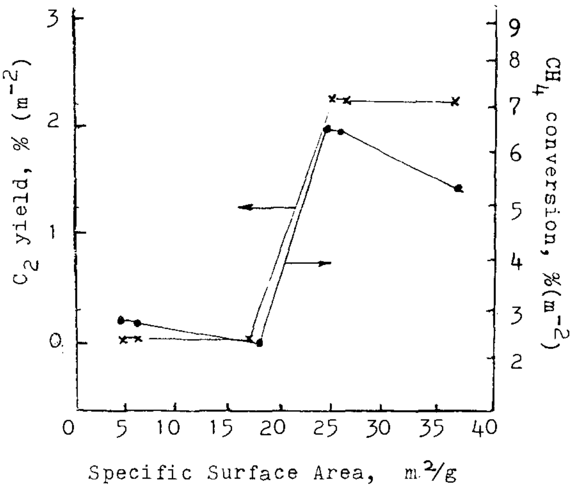

Fig. 5. Dependence of CH_4 conversion (m^{-2}) and C_2 yield (m^{-2}) on specific surface area.

is lower, the formation rate of $CH_3\cdot$ radicals is faster than that of complete oxidation of methane, so the catalyst with larger surface area has higher methane conversion. If the catalyst surface area is larger and the temperature is higher, the formation rate of $CH_3\cdot$ radicals is slower than that of complete oxidation of methane, the larger surface area is unfavorable to methane conversion.

At lower temperatures and in relatively smaller surface area range CH_4 conversion, C_2 yield and selectivity are in line with catalyst surface area. The phenomenon that CH_4 conversion, C_2 yield and selectivity are in line with selectivity decrease with the increase of surface area as shown in some references only occurs at higher temperatures for the catalysts with very high surface area. For MgO catalysts, in this paper, the surface areas are not very large, so at lower temperatures the larger surface area is beneficial to methane conversion and coupling. The optimum temperature range for MgO catalysts is 923–973 K.

3.2. XRD MEASUREMENT

MgO has face cubic centered structure. There are three characteristic diffraction peaks at 35–60° (2θ). The XRD patterns indicate that diffraction intensity is different for the catalysts prepared by different methods. Their lattice parameter, crystal dimension, lattice distortion and relative diffraction intensity are presented in table 1. It is found that the catalysts with larger diffraction intensity have larger crystal dimensions.

From the surface area formula $S = 6/\rho D_{hkl}$ it is clear that the catalyst with larger crystal dimension provides smaller surface area. This result is consistent with that obtained with the air adsorption method.

The lattice distortion also provides similar information, i.e., the trend of the lattice distortion is in good agreement with that of CH_4 conversion. The catalysts with larger lattice distortion have higher CH_4 conversion and vice versa. The lattice distortion is related to the amounts of lattice defect in the bulk of catalysts. It may not only cause the change of surface area but also the lattice distortion influencing the catalytic properties.

Comparatively, the effect of lattice parameter on the catalytic activity is not apparent. The lattice parameter influences the bulk structure and then the catalytic properties indirectly, i.e., through the lattice dimension and lattice distortion.

Table 1
Structure parameters of different MgO oxides for samples A–F

	A	B	C	D	E	F
a (Å)	4.2155	4.3151	4.2147	4.2137	4.2165	4.2198
D_{200} (Å)	422	750	1126	1502	676	376
$\langle \varepsilon^2 \rangle^{1/2} \times 10^4$	6.0	3.0	1.0	0.8	1.7	3.2
I_X/I_A [a]	1.0	2.4	3.1	3.1	2.7	2.1

[a] I_A: intensity of (200) of sample A; I_X: intensity of (200) of samples A–F.

Table 2
XPS data of MgO before reaction

Sample	C_{1s}		O_{1s} [a]					Mg_{2p}	
	(eV)	(%)	l (eV)	(%)	u (eV)	(%)	total (%)	(eV)	(%)
A	289.9	1.5	529.4	1.5	531.2	53.0	54.5	49.3	44.0
B	289.7	2.4	529.5	16.1	531.5	31.4	47.5	49.1	50.1
C	289.4	1.9	529.7	28.8	531.7	18.6	47.4	49.1	50.7
D	289.7	2.3	529.5	23.0	531.7	24.1	47.1	49.1	50.6
E	289.4	0.9	529.4	20.6	531.4	25.5	46.1	49.2	53.0
F	289.4	2.3	529.4	13.1	531.4	31.3	44.4	49.2	53.2

[a] l: lattice oxygen; u: unsaturated coordinated oxygen.

3.3. XPS MEASUREMENTS

The binding energy of O_{1s}, C_{1s} Mg_{2p} and their atomic percentage on the surface of the samples are listed in table 2. Two kinds of oxygen species with different E_b are assigned to lattice oxygen (at low energy) and unsaturated coordinated oxygen (at relatively high energy), respectively. The relative ratio of these two surface oxygens is given as well. Fig. 6 shows the relation between the atomic percentage of both oxygen surface species and the methane conversion of samples. It seems very clear that the lattice oxygen and the unsaturated coordinated surface oxygen have opposite effect on the methane conversion. Based on the above discussion one can conclude that the unsaturated surface oxygen is beneficial to methane activation.

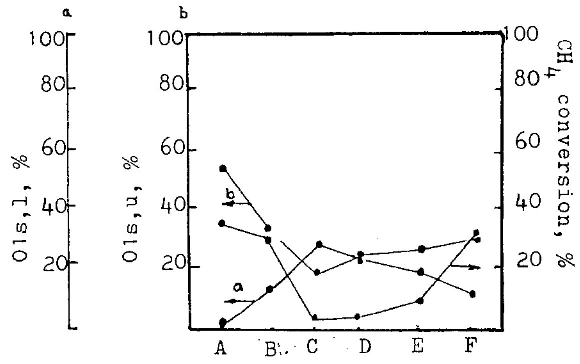

Fig. 6. Dependence of CH_4 conversion (923 K) on O_{1s}, l (%) and O_{1s}, u (%) for different MgO.

Acknowledgement

This work was supported by The National Natural Science Fund China.

References

[1] K. Aika, T. Moriyama, N. Takasaki and E. Iwamatsu J. Chem. Soc. Chem. Commun. (1986) 1210.
[2] J.A.H. Pol, S. Badyal, X.K. Zhang and R.M. Lambert, Surf. Sci. Lett. 225 (1990) L15.
[3] J.H. Lunsford, J.X. Wang and D.J. Driscoll, J. Am. Chem. Soc. 107 (1985) 58.
[4] K. Otsuka and K. Jinno, Inorg. Chem. Acta 121 (1986) 237.